

## Journal Pre-proof

Toxicological effects of three different types of highly pure graphene oxide in the midge *Chironomus riparius*

Raquel Martin-Folgar, Adrián Esteban-Arranz, Viviana Negri, Mónica Morales



PII: S0048-9697(21)07543-4

DOI: <https://doi.org/10.1016/j.scitotenv.2021.152465>

Reference: STOTEN 152465

To appear in: *Science of the Total Environment*

Received date: 20 September 2021

Revised date: 10 November 2021

Accepted date: 12 December 2021

Please cite this article as: R. Martin-Folgar, A. Esteban-Arranz, V. Negri, et al., Toxicological effects of three different types of highly pure graphene oxide in the midge *Chironomus riparius*, *Science of the Total Environment* (2021), <https://doi.org/10.1016/j.scitotenv.2021.152465>

This is a PDF file of an article that has undergone enhancements after acceptance, such as the addition of a cover page and metadata, and formatting for readability, but it is not yet the definitive version of record. This version will undergo additional copyediting, typesetting and review before it is published in its final form, but we are providing this version to give early visibility of the article. Please note that, during the production process, errors may be discovered which could affect the content, and all legal disclaimers that apply to the journal pertain.

© 2021 Published by Elsevier B.V.

## Toxicological effects of three different types of highly pure graphene oxide in the midge *Chironomus riparius*

Raquel Martin-Folgar<sup>a,\*†</sup>, Adrián Esteban-Arranz<sup>b †</sup>, Viviana Negri<sup>c</sup>, Mónica Morales<sup>a</sup>

<sup>a</sup> Grupo de Biología y Toxicología Ambiental, Departamento de Física Matemática y de Fluidos, Facultad de Ciencias, UNED. Urbanización Monte Rozas, Avda. Esparta s/n, Crta. de Las Rozas al Escorial Km 5, 28232, Las Rozas (Madrid), Spain.

<sup>b</sup> Departamento de Ingeniería Química de la Universidad de Castilla la Mancha (UCLM), Avda. Camilo José Cela, 12, 13071, Ciudad Real, Spain.

<sup>c</sup> Departamento de Ciencias de la Salud de la Universidad Europea de Madrid (UEM), C/ Tajo, Villaviciosa de Odón, 28670, Madrid, Spain.

† These authors contributed equally to this work.

\*Corresponding author. Tel: +34 913987124. E-mail: mfolgar@ccia.uned.es (Raquel Martín Folgar)

### **Abstract**

Graphene oxide (GO) is a carbon nanomaterial used in electronics, biomedicine, environmental remediation and biotechnology. The production of graphene will increase in the upcoming years. The carbon nanoparticles (NPs) are released into the environment and accumulated in aquatic ecosystems. Information on the effects of GO in aquatic environments and its impact on organisms is still lacking. The aim of this study was to synthesise and characterise label-free GO with controlled lateral dimensions and thickness – small GO (sGO), large GO (lGO) and monolayer GO (mlGO) – and determine their impact on *Chironomus riparius*, a sentinel species in the

freshwater ecosystem. Superoxide dismutase (SOD) and lipid peroxidation (LPO) was evaluated after exposures for 24 h and 96 h to 50, 500, and 3,000  $\mu\text{g/L}$ . GOs accumulated in the gut of *C. riparius* and disturbed its antioxidant metabolism. We suggest that all types of GO exposure can upregulate of SOD. Moreover, both IGO and mIGO treatments caused LPO damage in *C. riparius* in comparison to sGO, proving its favourable lateral size impact in this organism. Our results indicate that GOs could accumulate and induce significant oxidative stress on *C. riparius*. This work shows new information about the potential oxidative stress of these NMs in aquatic organisms.

Keywords: Graphene oxide; Ecotoxicology; Oxidative stress; *Chironomus riparius*

## **1. Introduction**

Nanotechnology is a new and broad field of science that focuses on the use of nano-sized materials, with one dimension in the size range of 1–100 nm (“No Title,” n.d.) Carbon-based materials (CBM) have unique properties (high surface area and strength as well as easy surface modification capability, among others) and are considered as promising materials for biomedicine, biotechnology, and wastewater treatment technologies (Castillejos et al., 2020; Chen et al., 2021; Scida et al., 2011; Zhang et al., 2021). Water and soil are the major environmental receptors of nanomaterials (NMs). The different routes to synthesise these CBM are expected to increase in the following years. Consequently, this massive production of CBMs will imply an increase in the exposure of these nanoparticles (NPs) in humans as well as in different organisms. In addition, many CBM have been incorporated into consumer products (Vance et al., 2015).

Graphene is a CBM that was isolated by Andrea Geim and Konstantin Novosolov in 2010, considered as a 2D material with a flat sheet structure (Peres et al., 2006). The

production of different conformations and types of graphene-based materials (GBM) – such as few-layer graphene, multi-layer graphene, graphene nanosheets, graphene oxide (GO), and reduced GO (rGO) – has increased worldwide (De Marchi et al., 2018; Esteban-Arranz et al., 2018; Jastrzębska et al., 2012). GO represents one of the most promising GBM for water-based applications (Zhang et al., 2021) given the incorporation of different oxygen functional groups at the basal plane and edges (de Lázaro et al., 2019). GO is obtained by different synthetic routes; however, the most common one is based on oxidising the bulk graphite and then separating each GO layer, obtaining a flat oxidised material (Benzait et al., 2021; Marcano et al., 2010; Zaaba et al., 2017). During this process, some oxygen functional groups such as epoxide, hydroxyl, and carboxyl groups are incorporated (Bianco et al., 2013; De Marchi et al., 2018). These oxygenated functional groups endow it with the possibility of getting dispersed in aqueous solutions. The hydrogen bonds between polar functional groups presented on the GO surface and water molecules leads to a stable colloidal suspension (Shih et al., 2012). GO presents a more hydrophilic nature in comparison to the rest of GBM (Esteban-Arranz et al., 2021) because of its high oxygen content, being stable in aquatic ecosystems (Compton and Nguyen, 2010). Previous studies show that GOs fate and transport are influenced by environmental conditions. Studying the environmental GOs behaviour is essential to predict their effects. The GO stability is influenced by aquatic environment physical-chemical properties (pH, natural organic matter (NOM), divalent cations, etc.) and can modify their colloidal properties (He et al., 2017).

In a review recently published about the impact of GBM on the aquatic environment, it was highlighted that the structure and surface properties of GO materials – such as the lateral size, the C/O ratio, and the structural defects – influenced the different colloidal behaviours, adsorption capabilities, and toxicities of GO (Zhao et al., 2014).

*Chironomus riparius* is one of the most abundant Diptera species in aquatic systems (Rasmussen, 1985) and represents one of the key elements in the trophic chain of aquatic ecosystems (Berg and Hellenthal, 1992). They constitute a part of the diet of different terrestrial and aquatic organisms, mainly fish and waterfowl. (Rieradevall M, 1995). The benthic communities, in which the chironomids constitute one of the most abundant macroinvertebrates, are sensitive to changes in water and sediment conditions, which are excellent environmental indicators to assess hydrological alterations and the impact of pollutants (OECD, 2011, 2004). This species has been commonly used in ecotoxicity studies and as a bioindicator of water quality and is considered as a reference organism (Rasmussen, 1985). Organizations such as the U.S. Environmental Protection Agency have published standardized protocols for toxicity testing with these insects (“ASTM International. 2006. Standard guide for conducting acute toxicity tests on test materials with fishes, macroinvertebrates, and amphibians. E729-96 (2002),” 2006; OECD, 2011, 2004; United States. Environmental Protection Agency. Office of Prevention, 1996). The interactions between *C. riparius* and CBM have been poorly studied, and the information on their effects is scarce (Martínez-Paz et al., 2019; Waissi et al., 2017). Previous studies with other species of aquatic invertebrates have shown that GO could induce acute toxicity, bioaccumulation, and oxidative stress [20–22]. They also indicated that nanomaterials could compromise antioxidant metabolism (Wu et al., 2010). When the antioxidant systems are properly the homeostatic stability is maintained. This allows organisms to succeed the toxic caused by reactive oxygen species (ROS) (Lushchak et al., 2005). On the other hand, antioxidant systems may not be sufficient in the presence of high concentrations of xenobiotics, leading to alterations in important molecules such as membrane lipids and nucleic acids [27, 28]. Therefore, enzymatic biomarkers may be useful in environmental ecotoxicology studies, as they

provide information to understand the mechanisms of toxicity (Ighodaro and Akinloye, 2018)

The aim of this study was to synthesise and characterise different GO materials – small GO (sGO), large GO (lGO), and monolayer GO (mlGO) – that are currently being used in different areas of industry and evaluate their toxicological effects. The effect of these GO solutions was evaluated in the larvae of *C. riparius* after 24 and 96 h of exposure. In addition, to our knowledge, thorough research on the uptake in the digestive tract of GO in *C. riparius* as a model organism has not previously been established. This research is the first study to analyse the impact of the different physicochemical properties of GO solutions as well as their thickness and lateral size on the toxicological effects in this aquatic organism, paying special attention to their antioxidant metabolism.

The entry of GO into the environment and consumer products obliges evaluations in addition to the need to study their potential impact on human health. The need to define GO-induced environmental effects in sentinel organisms and to develop approaches towards measuring endpoint outcomes is urgent.

## ***2. Materials and methods***

### ***2.1. Synthesis and characterisation of GO materials***

Large GO (lGO) was synthesised following a previous study published by Jashim et al. (Jasim et al., 2016) based on the Hummers modification method. Graphite powder purchased by Sigma Aldrich was mixed with  $\text{H}_2\text{SO}_4$  and  $\text{NaNO}_3$  in an ice bath. Then,  $\text{KMnO}_4$  was slowly incorporated until a homogeneous green solution was produced. After that, water was drop by drop added to the solution, monitoring its temperature. The mixture was left to stir at 98 °C for 30 minutes. Then,  $\text{H}_2\text{O}_2$  was added to stop the

reaction and left to settle. The following day after the synthesis, IGO was separated from the graphitic carbon residue and purified via centrifugation (8,800  $\times g$ , 25 min). Recently, Esteban-Arranz et al. (ESTEBAN-ARRANZ et al., 2021) found that the washing fraction prior to the solubilisation of the orange gel contained mlGO flakes. Thus, they were collected and characterised to evaluate the thickness of these materials in this research. Additionally, to assess the effect of their lateral size, sGO was produced following the methodology published by Rodrigues et al. (Kostarelos, 2018).

The thickness and lateral dimensions of the materials were defined by atomic force microscopy (AFM) (Nanoscope VIII - FESP cantilever tip, tapping mode Bruker). Prior to the deposition of GO, exfoliated mica was functionalised by 0.01% of positively charged poly-L-lysine (20  $\mu\text{L}$ ). After two minutes in contact with the surface of the mica, the excess was washed off with water. Then 20  $\mu\text{L}$  of the GO solution (100  $\mu\text{g}\cdot\text{mL}^{-1}$ ) was gently dispersed on the surface of the mica. After two minutes, the sample was washed again to avoid agglomerations and placed into an oven at 40°C overnight. Scanning transmission electron microscopy was also used to determine the lateral dimensions of the flakes (GeminiSEM 500 in STEM mode, ZEISS). Additionally, the structural and morphological features of these materials were defined by high-resolution scanning electron microscopy (HRSEM) (GeminiSEM 500, ZEISS). Raman experiments were carried out to define the degree of defects (Renishaw in Via spectrometer, 633 nm 0.1% power laser and 50x). Spectra were recorded from 1,000 to 3,250  $\text{cm}^{-1}$ . For the analysis of the results, the spectra were normalised by the intensity of graphitic (G) (OriginPro 8.5 software). X-ray diffraction experiments were conducted to define their structural features (Philips X'Pert MPD diffractometer, Cu  $K\alpha 1$  (1.54056 Å) radiation at 40 mA, 40 kV). Colloidal stability in the culture media of *C. riparius* for 24 h was defined (Turbiscan Lab Expert stability analyser). GO dispersions (3,000  $\mu\text{g}\cdot\text{mL}^{-1}$ ) were placed in a cylindrical vial (30 mL) prior to their measurement. The results were presented as Turbiscan Stability Index (TSI) values. The surface chemistry of the GO materials was elucidated via Fourier transform infrared (FTIR) spectroscopy (Spectrum Two FTIR spectrometer, zinc selenide (ZnSe) crystal, PerkinElmer).

The spectra range was set from 4,000 to 4500  $\text{cm}^{-1}$  with 4  $\text{cm}^{-1}$  resolution and 150 scans per sample.

## **2.2. Animals and culture**

Fourth instar larvae of an aquatic midge *C. riparius* were used in the experiments. The cultures were maintained according to toxicity testing guidelines (OECD, 2011) at 20°C and a standard light–dark period (16L:8D). For the experimental exposures, the larvae were treated to different types of GO NPs diluted in the culture medium for 24–96 h (Martínez-Paz et al., 2019).

## **2.3. Ecotoxicity tests**

Observations on larval survival were made after 24, 48, 72, and 96 h. Individuals were considered dead when they did not move. (immobility / mortality of the organisms). For treatments, the larvae were exposed to 10, 50, 200, 500, 1,000, and 3,000  $\mu\text{g/L}$  of sGO, lGO, and mlGO for up to 96 h in glass recipients (200 mL), covered with aluminium foil to avoid photodecomposition. Commercial fish food (3 mg) per replicate was provided every 48 h. Each treatment was carried out in triplicates of 30 larvae and three independent experiments performed in each analysis using samples from three different egg masses. The controls were only exposed to the culture medium. Exposure media were not renewed during the assay.

## **2.4. Graphene oxide treatments**

The *C. riparius* fourth instar larvae were exposed to 0 (control), 50, 500, and 3,000  $\mu\text{g/L}$  of sGO, lGO, or mlGO for 24 and 96 h. The stocks solutions of GOs were prepared in reconstituted water at concentration of 300  $\mu\text{g/mL}$ . These stocks solutions



were diluted in culture medium at the concentrations used in the acute and chronic exposures. Three independent experiments were performed using 10 organisms per replicate (n = 30) of different egg masses.

## ***2.5. Analysis of uptake in *C. riparius****

The uptake of GO in *C. riparius*, was done with a digital camera (Nikon D810). Macro observations allowed us to test the possible internalization of the larvae exposed to 10, 50, 200, 500, 1,000 and 3,000 µg/L of different types of GO solutions (sGO, lGO, and mGO), for 24 and 96 h, compared to controls.

## ***2.6. Biochemical analyses***

### ***2.6.1. Antioxidant enzymatic activities of superoxide dismutase***

The antioxidant enzymatic activities in response to sGO, lGO, and mGO were measured after 24 and 96 h exposure to 50, 500, and 3,000 µg/L. Larvae were homogenised in 0.4 mL of a phosphate buffer (22 mM KH<sub>2</sub>PO<sub>4</sub>, 4.2 mM Na<sub>2</sub>HPO<sub>4</sub>, and 86 mM NaCl, pH 7.2) with a pellet mixer (VWR, part of Avantor). The homogenate was centrifuged for 10 min at 10,000 g at 4°C. Total protein was quantified with a BCA protein assay reagent (Thermo Scientific), and 10 µg of the protein was used for the superoxide dismutase (SOD) assay. SOD activity was determined with a commercial kit (Sigma-Aldrich). The SOD activity was evaluated as an inhibition activity by measuring the decrease in colour development at 450 nm.

### ***2.6.2. Antioxidant enzymatic activities of lipid peroxidation***

Lipid peroxidation (LPO) was evaluated using a commercial LPO (MDA) assay kit (Sigma-Aldrich) by measuring the MDA levels. MDA is detected at 532 nm.

## ***2.7. Statistical analysis***

The normalised levels of SOD and LPO in the treated larvae were compared with controls using ANOVA. Dunnett's multiple comparison tests were then performed with SPSS 24 software (IBM, USA). Normal distribution and variance homogeneity were assessed with the Shapiro-Wilk and Levene tests, respectively.

### ***3. Results and discussion***

Due to the increase in graphene products, it is to be expected that GO-based materials will be released into the environment in the process of manufacture, transport, use and disposal. Once present in aquatic ecosystems, sediments and soils, they interact with physicochemical and biological factors. NMs are included in the Registration, Evaluation, Authorisation, and Restriction of Chemicals' (REACH) definition of 'substance', but no specific reference to these materials exists. The general REACH obligation for nanomaterials is the same as that for other substances. It is therefore necessary to understand the environmental risks of the different GO solutions currently used in different areas of industry. Although the cellular toxic effects of exposure to graphene and its derivatives (GO) have been assessed in recent years (Malhotra et al., 2020), the lack of knowledge about their ecotoxicity is significant. Thus, it is a priority to conduct studies on their behaviour in aquatic ecosystems so as to establish their adverse effects and their possible mechanisms of toxicity.

#### ***3.1 Characterisation of graphene oxide material***

Unveiling the possible relationship between different sizes of GOs and the associated toxicological impacts on different biological systems (invertebrates, human cells, zebrafish, etc.) is of vital importance to assess potential environmental risks and ensure a safe and responsible use of these NMs. Therefore, it is necessary to perform a pre-

exposure characterization in an experimental model. Previous studies suggest that the physical-chemical characteristics of nanomaterials could be related to a different toxicological potential (Li et al., 2021), which would imply a different effect at the individual and therefore ecosystem level. Sizes and surface oxidation of GrO nanomaterials potentially affect their properties and associated toxicity on various models in vitro and in vivo (Linares et al., 2014; Wibroe et al., 2016; Yang et al., 2012)

A group of characterization techniques has been applied to define the physicochemical properties of these GO materials. Lateral dimensions and thickness profiles have been defined by STEM and AFM analyses. Their morphology has been elucidated by SEM micrographs. Additionally, their structural features have been determined by XRD and Raman analyses. The impact of their physicochemical properties on their colloidal stability has been figured out by Turbiscan experiments, and FTIR experiments have been carried out to establish their surface chemistry.

The AFM analyses of the different GO materials with their respective thickness profiles and STEM micrographs are shown in Figure 1 (A) and (B), respectively. All the GOs present flake-shape morphology. Figure 1 shows bigger flakes for the lGO (~10  $\mu\text{m}$ ) and mlGO (~9  $\mu\text{m}$ ) materials in comparison to the sGO material (~500 nm). Otherwise, based on their thickness profiles, mlGO (~0.66 nm) presents thinner structures than lGO (~4 nm). These results demonstrated the presence of mlGO flakes in the case of mlGO and few-layer GO ( $n < 10$ ) for lGO. Our lateral size and thickness results are in agreement with the values reported by Rodrigues and Esteban-Arranz since mlGO presents thinner structures than and similar lateral dimensions to lGO.

HRSEM micrographs were acquired to reveal the morphology of the resulting GO materials; the results are shown in Figure 2 (A). Graphite oxide (GrO) is also

incorporated for comparison purposes. All the materials display flat structures, as characteristic of GBM. In the case of GrO, a wrinkled surface and multiple layers are detected. Thinner GO materials are produced after mechanical separation during the purification step in the synthesis process. The sGO layers seem to display smaller lateral dimensions than those of IGO, which is in agreement with our previous results. In addition, mlGO presents a more analogous lateral dimension than IGO but with thinner layers, as demonstrated by the AFM and STEM experimental outcomes.

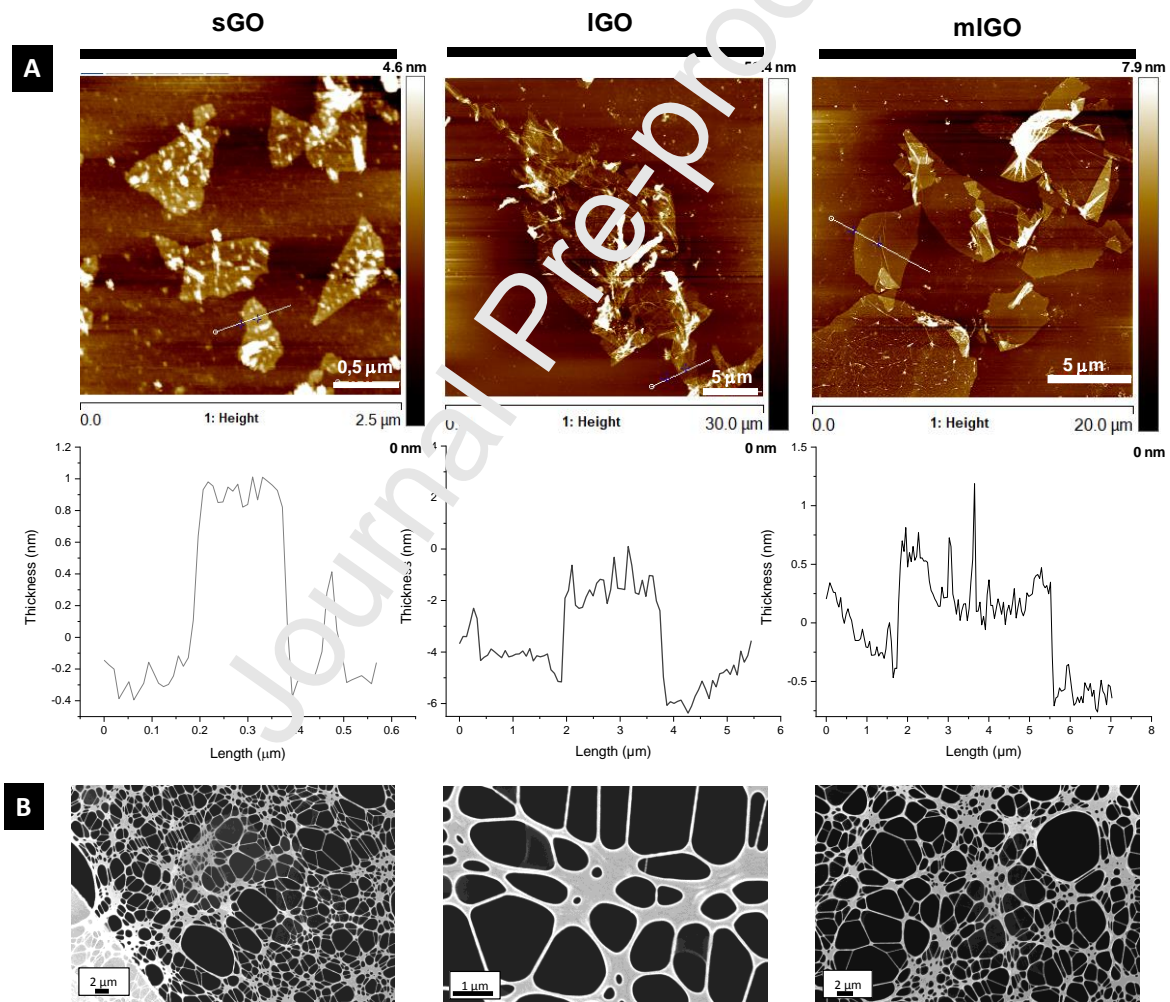


**Figure 1.** AFM analyses and thickness profiles of sGO, IGO, and mlGO (A) and their STEM micrographs (B).

XRD and Raman experiments were carried out to establish the structural characteristics of these GO materials. The XRD diffractograms are plotted in Figure 2 (C). sGO and

lGO show well-defined peaks of the (001) plane. After the oxidation treatment, the graphitic (002) plane shifted to lower  $2\theta$  values because of the incorporation of water molecules and oxygen functional groups between their layers. In the case of mlGO, this peak was not clearly detected, showing its high exfoliated character. Figure 2 (D) compiles the Raman spectra of the different materials. The ratio between their intensity bands ( $I_D/I_G$ ) has been previously established as a parameter to determine the degree of defects presented in these materials. The results of their  $I_D/I_G$  values demonstrate (1.30–1.40) that they can be considered as low-defect graphene materials based on the classification of Lopez-Diaz (López-Díaz et al., 2017). The mlGO material presents a lower degree of defects in comparison to those of sGO and lGO.

One of the main properties of materials being used in biomedicine or water-based applications is their colloidal stability in aqueous media. Therefore, stability experiments in the culture media of *C. riparius* of the different GO materials were carried out for 24 h; the results are depicted in Figure 2 (B). To ensure that the concentration of the material in the solution was detectable for the apparatus, the culture media alone, as a blank experiment, was previously tested. Based on the classification of Dai et al., three different regions depending on the TSI values can be established. Materials with good dispersion capacities show a  $TSI < 5$ . If the material is deposited at the bottom of the flask but can be easily re-dispersed, its TSI value will range from 5 to 20. Otherwise, non-redispersable materials will show TSI values  $> 20$  (Dai et al., 2015). The results obtained show the good dispersion capacity of the materials in this aqueous culture media ( $TSI < 5$ ). The incorporation of oxygen functional groups at the basal plane and edges facilitates the dispersion of these CBM in aqueous media. In a decreasing order of stability, the following trend was detected – *lGO* (4.15) < *sGO* (3.20) < *mlGO* (2.65). Multiple studies have shown better dispersion of smaller flakes

in comparison with the bulk material (Szabo et al., 2020). Based on these experimental outcomes, we postulate that the thickness of the material is a more critical physical parameter than the lateral dimension for colloidal applications in this culture media. Esteban-Arranz et al. found similar results in aqueous media.

The surface chemistry of these materials was defined via FTIR analyses. A wide band referred to the stretching vibrations of hydroxyl groups is detected between 3,690 and 2,915  $\text{cm}^{-1}$ . The presence of these hydroxyl groups is corroborated by the hydroxyl band at 1,377  $\text{cm}^{-1}$ . Otherwise, the band presented at 1,717  $\text{cm}^{-1}$  is related to the carbonyl stretching vibrations in the carboxylic group. The band centred at 1,600  $\text{cm}^{-1}$  is characteristic of the aromatic stretching vibration with vicinal hydroxyl groups on acidic surfaces. Finally, the sharp band found at 1,065  $\text{cm}^{-1}$  is related to the C-C skeleton (Țucureanu et al., 2016).

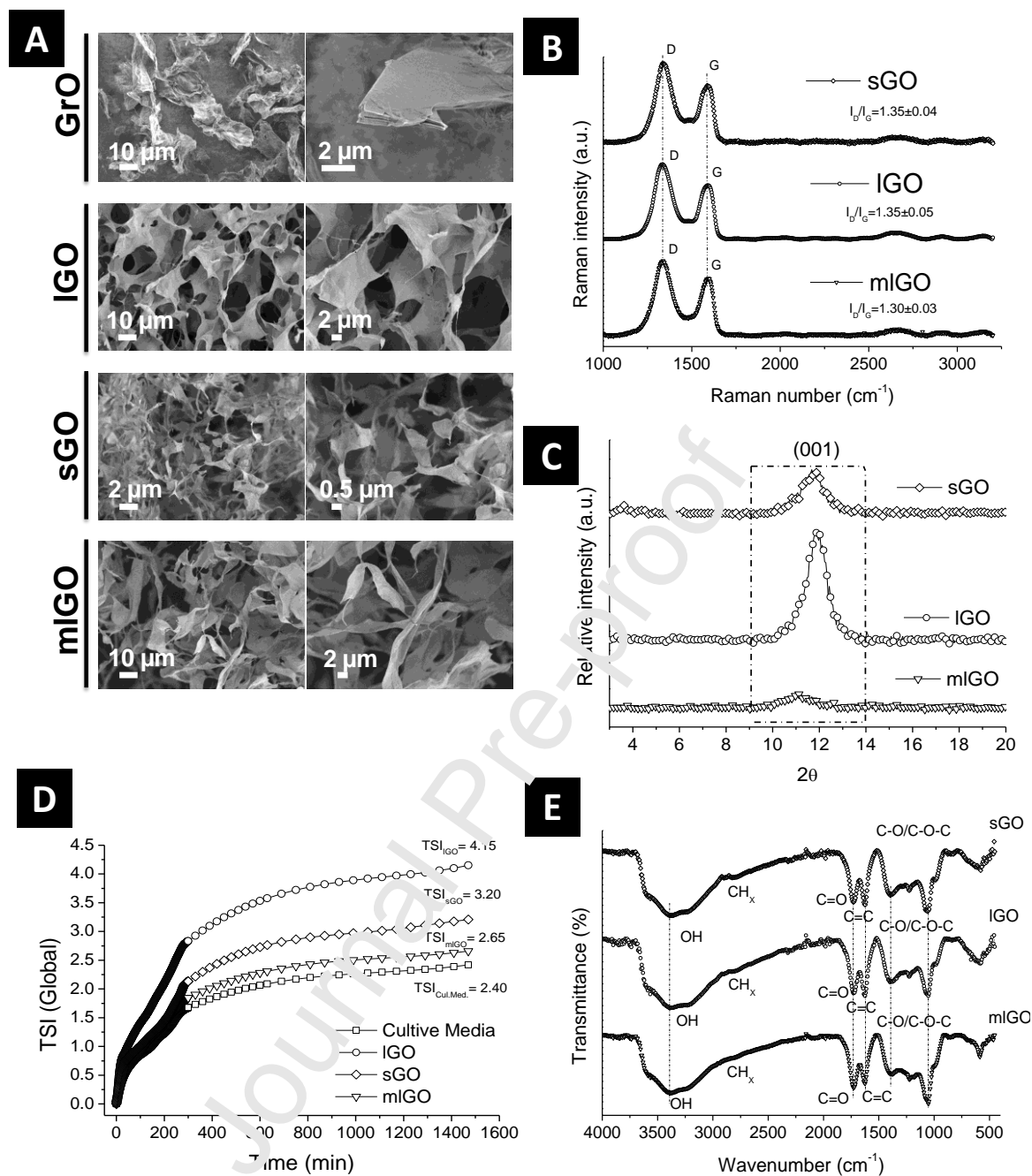


**Figure 2.** HRSEM micrographs of GrO, IGO, sGO, and mlGO (A). Raman (B) and XRD (C) structural results of the stability experiments at 3,000  $\mu\text{g/mL}$  in *C. riparius* culture media for 24 h (D) and their surface chemistry via FTIR (E).

All the materials present the same surface chemistry; however, mlGO shows more contribution of oxygen functional groups, which may be due to fewer GO layers.



### 3.2. *In vivo* graphene oxide exposures and larval survival

To know the aquatic toxicity of sGO, lGO, and mlGO, the mortality of *C. riparius* under these nanomaterials' exposure was examined. Studies regarding the toxicity of GO towards aquatic organisms are scarce and limited (Malhotra et al., 2020). The presence of sGO, lGO, and mlGO in the medium of *C. riparius* did not affect larval mortality. The larvae maintained normal appearance, behaviour, and motility. The sGO, lGO, and mlGO treatments showed low toxicity to *C. riparius* fourth instar larvae, with a survival rate between 80% and 90%. It should be noted that the concentrations of sGO had the lowest percentage of mortality. The results obtained show non-significant increased mortality in larvae exposed to mlGO from the 24 h treatments (data not shown). The treatments at concentrations of 10, 50, and 200 µg/L of sGO presented the lowest percentage of mortality (Table 1). The data showed higher mortality in larvae exposed to mlGO > lGO > sGO. Smaller and thicker GO flakes (sGO) provoked less mortality of *C. riparius* in comparison to thinner and bigger GO flakes (mlGO). Previous works reported that GO was either nontoxic (Chen et al., 2012; Liu et al., 2011) or considerably toxic (LIU Xiao Tong, 2014) to embryos of *Danio rerio*, nontoxic to the algae *Chlorella vulgaris* (Wahid et al., 2013), to the algae *Euglena gracilis* (Hu et al., 2015), to the shrimp *Artemia salina* (Mesarič et al., 2015), and to *Daphnia magna* (Lv et al., 2018). Moreover, De Melo (2019) (Batista de Melo et al., 2019) reported that GO did not produce toxicity at a concentration of up to 5.0 mg/L after 96 h treatment in *Palaemon pandaliformis*.

Larvae exposed to the higher GO concentrations for 72 and 96 h appeared very yellowish. Larval discoloration can be due to the decrease of red pigmentation, typically associated with haemoglobin (Hb), which has been used as one of the bio-indicators of



exposure to pollutants on *Chironomidae*. (Choi and Ha, 2009; MacDonald et al., 2004; Majumdar TN, 2012). The natural population of *Glyptotendipes* spp. and *Endochironomus* spp. exposed to heavy metal contamination revealed a significant reduction in the level of Hb protein (De Coursin Jacobs, 2006). The expression of the Hb gene was a modulated form of herbicide treatment (Anderson et al., 2008). Recently, one study showed the effects of metal oxide nanomaterials on *C. riparius* impacting Hb levels and heme metabolism genes (Niemuth et al., 2019). Much effort is still needed to understand the impact of GO on the Hb of *Chironomus* spp. in the freshwater ecosystem, where the population is subjected to more than one environmental stressor.

**Table 1.** Ecotoxicity effects on *Chironomus riparius* after exposure to GO solutions (96 h). No mortality was detected in the control group.

Concentration ( $\mu\text{g/L}$ )	Immobility/mortality			Total organisms	Mortality effect (%)		
	sGO	IGO	mlGO		sGO	IGO	mlGO
<b>10</b>	4	9	15	90	4%	10%	17%
<b>50</b>	7	9	21	90	8%	10%	23%
<b>200</b>	2	11	13	90	2%	12%	14%
<b>500</b>	10	10	11	90	11%	11%	12%
<b>1,000</b>	13	13	18	90	14%	14%	20%
<b>3,000</b>	9	12	11	90	10%	13%	12%

### 3.3. GO uptake

GO materials are dispersed in water. This implies their uptake by aquatic animals and aggravates their hazards after bioaccumulation. In this study, *C. riparius* has shown noticeable internalization of sGO, IGO, and mlGO in the digestive tract. After 24 h of exposure, only the 3,000  $\mu\text{g/L}$  concentration of sGO, IGO, and mlGO compounds

accumulated mainly in the *C. riparius* digestive tract (Figure 3). On the other hand, exposures of all concentrations and materials for 96 h to *C. riparius* showed the presence of GO in the digestive tract (Figure 4). These results demonstrated that *C. riparius* can take up GO materials from the culture medium, the gut tract being one of the organs where these materials accumulate in this organism. NMs can enter aquatic organisms through their gills and digestive tracts (Zindler et al., 2016).

The accumulation of GO in aquatic invertebrates is relevant because these organisms are the basis of the trophic chain. Therefore, accumulation of GO in higher organisms should be expected (Cano et al., 2018). NPs accumulation was also observed in other aquatic invertebrates for other carbon nanomaterials (single walled carbon nanotubes, carbon black and nanodiamonds) in *Daphnia magna* (Mendonça et al., 2011; Petersen et al., 2009; Sohn et al., 2015); for multi walled carbon nanotubes in *Ceriodaphnia dubia* (Li et al., 2011), *A. salina* (Zhu et al., 2017), and *C. riparius* (Martínez-Paz et al., 2019); and for different types of NPs of pristine graphene in *A. salina* (Pretti et al., 2014) and *C. dubia* (Souza et al., 2018).

The presence of GO in the digestive tract could persist in the long term. Previous studies show that accumulation in the digestive tract alters the function of the peritrophic membrane of the intestinal tract. This membrane supports digestive processes and protects the epithelium of the intestinal tract (Mendonça et al., 2011). The presence of GO may interfere with food intake and nutrient absorption, causing decreased feeding and reproductive rates (Mendonça et al., 2011). In addition, previous studies have revealed that NPs can cross the cell membrane without the need for any specific receptor-mediated interaction (Kettler et al., 2014; Lin et al., 2010; Lipowsky and Döbereiner, 1998; Zhang et al., 2015). Lipids are very flexible, and the bilayer can be deformed as a consequence of the adhesion of NPs to its surface, implying a total

uptake of the NPs. It appears that this uptake can be driven solely by physico-chemical interactions. Therefore, the uptake of these nanomaterials in organisms at the base of the food chain will lead to adverse effects on other higher organisms.

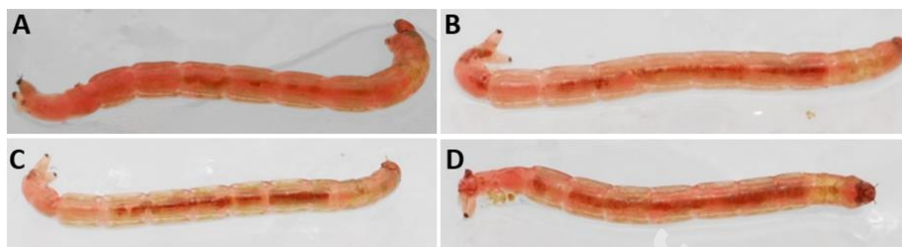


**Figure 3.** The presence of GO in the digestive tract of *C. riparius* larvae exposed to 3,000  $\mu\text{g/L}$  for 24 h. Control (A), sGO (B), IGO (C), and mlGO (D).

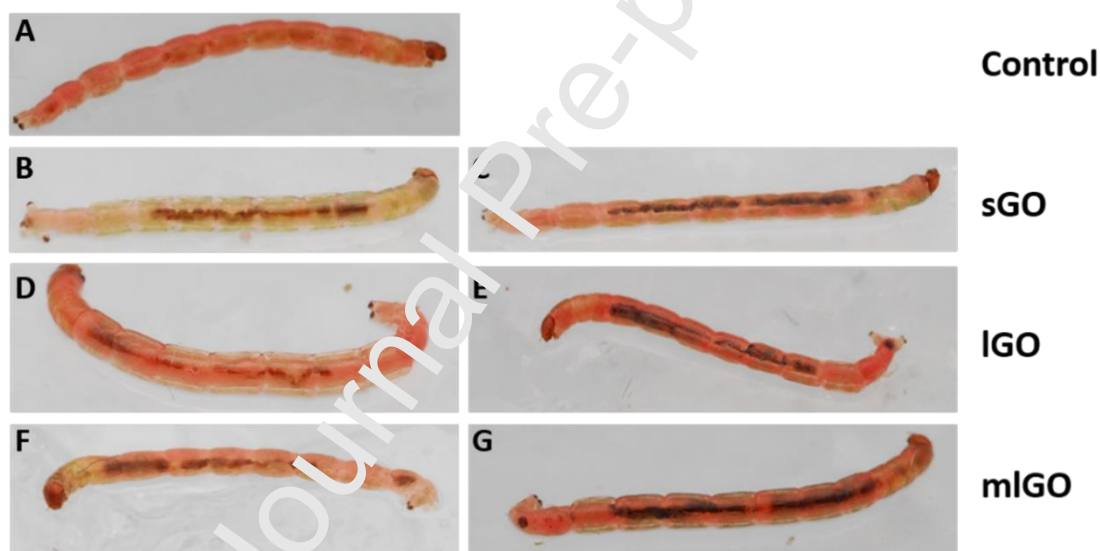


**Figure 4.** The presence of GO in the digestive tract of *C. riparius*. Control (A), 50  $\mu\text{g/L}$  of sGO (B), 3,000  $\mu\text{g/L}$  of sGO (C), 50  $\mu\text{g/L}$  of IGO (D), 3,000  $\mu\text{g/L}$  of IGO (E), 50  $\mu\text{g/L}$  of mlGO (F), and 3,000  $\mu\text{g/L}$  of mlGO (G) for 96 h.

### 3.4. Oxidative stress mediated by IGO, mlGO, or sGO

Studies on the toxicity of GO have increased in recent times, although few studies have focused on the implications of these NMs at the molecular and cellular levels. GO induces oxidative stress in bacteria (LIU Xiao Tong, 2014), algae (Hu et al., 2015), fish (Chen et al., 2016; Mu et al., 2015; Souza et al., 2021), and *D. magna* (Lv et al., 2018).

In this study, we have synthesised and characterised different types of GO solutions (sGO, IGO and mlGO) with potential use in biomedicine to study the effects they induce on *C. riparius* for the assessment of contaminated ecosystems (OECD, 2010). Here, we evaluate the response to these materials in *C. riparius* larvae and analyse the capacity of this aquatic invertebrate to manage the damage they cause.

In this study, we hypothesised that sGO, IGO, and mlGO produce oxidative stress in *C. riparius*. SOD activity and LPO content were measured to quantify oxidative stress. The defence antioxidants include SOD, catalase (CAT), and glutathione peroxidase (GPX). SOD is a detoxification enzyme antioxidant and a potent antioxidant in the presence of pollutants, including NMs and NPs (Chen et al., 2010; Ighodaro and Akinloye, 2018). CAT catalyses the degradation of H<sub>2</sub>O<sub>2</sub> to water and O<sub>2</sub> by SOD. GPX protects cells from oxidative stress (Ighodaro and Akinloye, 2018) playing a crucial role in inhibiting the LPO process. High oxidative stress can exceed antioxidant mechanisms and lead to oxidative damage that inhibits antioxidant activities (Zhu et al., 2011). LPO levels have been widely used as a biomarker of oxidative damage (Sayeed et al., 2003). Elevated peroxidative damage to unsaturated fatty acids can occur during oxidative stress (PANDEY et al., 2003). However, the inhibition of LPO has sometimes been documented in situations of cellular stress (Souza et al., 2019). The inhibition of the enzymatic oxidation of lipids can be achieved by inhibiting the activation or reaction of an enzyme. Free radical-mediated LPO can be inhibited by inhibiting chain initiation and propagation as well as accelerating chain termination. Singlet oxygen-induced LPO can also be inhibited (Niki et al., 2005).

In this study, sGO, IGO, and mlGO induced oxidative stress on *C. riparius*, especially at long exposure times (96 h) (Figures 5 and 6). Significant activation in SOD level were only showed after 24 h of exposure to IGO (50 and 3,000 µg/L). No change in SOD

activity was detected after 24 h of exposure to sGO and mlGO. All IGO concentrations tested (50, 500, and 3,000  $\mu\text{g/L}$ ) and the highest concentrations (500 and 3,000  $\mu\text{g/L}$ ) of mlGO caused significant increases in SOD activity (Figure 5) after 96 hours of exposure. An increase in the expression was observed with all the sGO concentrations, but it was not significant. In line with the LPO levels, peroxidative damage was not found with the sGO and mlGO treatments for 24 h and even with the sGO treatments at 96 h (Figure 5). The inhibition of LPO was observed after exposures to IGO at 50, 500, and 3,000  $\mu\text{g/L}$  at 24 h (Figure 6). On the other hand, peroxidative damage increased after 96 h of exposure to IGO at higher concentrations and mlGO at 50 and 500  $\mu\text{g/L}$ . Interestingly, inhibition was observed after treatment with mlGO at 3,000  $\mu\text{g/L}$ .

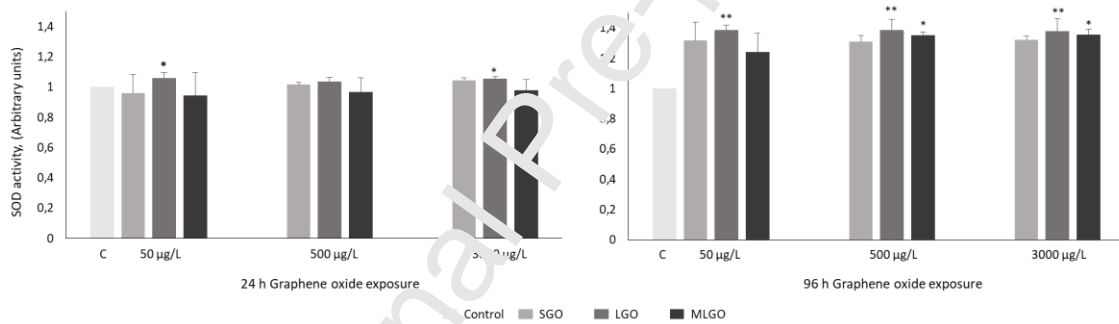


**Figure 5.** SOD activities on *Chironomus riparius* after 50, 500, and 3,000  $\mu\text{g/L}$  of sGO, IGO, and mlGO (\* $p < 0.05$ , \*\* $p < 0.01$ ).

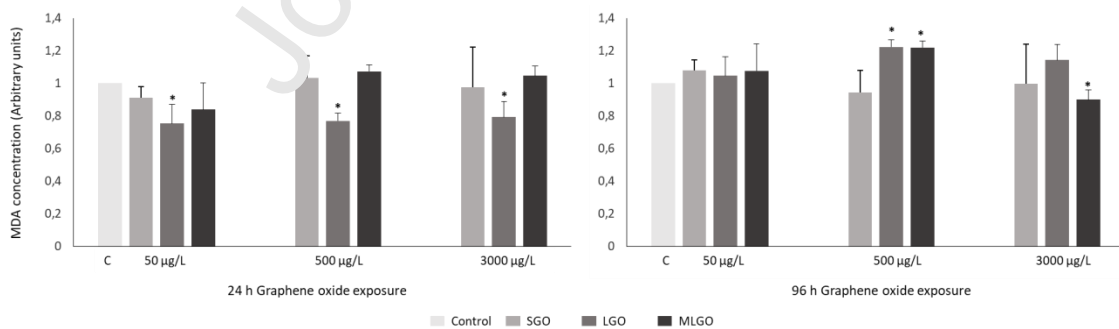


**Figure 6.** LPO on *Chironomus riparius* after 50, 500, and 3,000  $\mu\text{g/L}$  of sGO, IGO, and mlGO (\* $p < 0.05$ , \*\* $p < 0.01$ ). Lipid peroxidation was estimated by measuring the MDA levels.

An analysis of the pooled data showed that exposures of IGO and mlGO to *C. riparius* resulted in SOD activation. However, this enzyme and other antioxidant enzymes were

not sufficient to prevent the effects of ROS leading to LPO activation after 96 hours. Increased antioxidant metabolism in response to carbon NMs has been showed in other works (Souza et al., 2019; Zhu et al., 2017). These studies demonstrated the LPO inhibition (Chupani et al., 2018; Souza et al., 2019) after a period of recovery from nanomaterial exposure. The authors proposed that LPO levels decreased in an adaptive process, enhancing antioxidant defence. This adaptive response was enough to prevent LPO. Other studies report that some organisms may exhibit an adaptive response depending on the level, intensity, and nature of oxidative stress, in addition to the physiological state of the organism (Lushchak, 2011). The results of inhibition of LPO levels could indicate that *C. riparius* would be able to overcome the damage suffered during exposure. Further studies are needed to confirm this hypothesis. Organisms may have adaptive responses depending on their levels of oxidative stress. Previous studies on the recovery phase show that organisms can adapt to H<sub>2</sub>O<sub>2</sub> generated in cells using cellular mechanisms that facilitate tolerance to ROS (Lushchak, 2011). In addition, the cellular machinery would reduce the penetration of the toxicant, deactivating the toxicity of ROS through the antioxidant defence system.

Our results showed the first evidence that GO NPs can induce antioxidant defence in an insect after short-term exposure. The antioxidant response is very sensitive for the determination of the cause-effect relationship. Therefore, it is necessary to evaluate other endpoints in ecotoxicology (histological, molecular and oxidative stress generation parameters). Molecular-level studies on the potential effects of GO in invertebrates are scarce. Thus, further studies at the cellular and molecular levels on the effects of existing and emerging carbon nanomaterials on aquatic organisms are importance priority. In this way, the effects of these NMs on human and environmental health can be predicted.

## Conclusions

This work submits important information on the potential environmental consequences of GO exposure. The input of graphene oxide into the environment is expected to increase with the growth of its industrial applications. However, the impact of these nanomaterials on the environment and their ecological effects are so far very low. This is the first study on the possible toxic, uptake, and oxidative stress effects of label-free GO with three different types of lateral dimensions and thickness (sGO, lGO, and mlGO) in an insect model. The results revealed no toxicity of GO in *C. riparius*; however, GO absorption occurred in this organism. This would hypothesize the ability of *C. riparius* larvae to ingest and accumulate GO in the gut.

Another crucial outcome of this study was the observation of potential oxidative stress of these NMs. The results obtained from the biochemical analyses revealed a significant impact on antioxidant metabolism at the cellular level. This study displayed the potential of lGO and mlGO to affect *C. riparius* oxidative stress reactions after 96 h of exposure, mainly to the concentrations of 500 and 3,000  $\mu\text{g/L}$ . The effect depended on the GO concentration and exposure time. In contrast, the effects of sGO on the antioxidant metabolism of *C. riparius* were not as severe as those of the other two nanomaterials. This is consistent with toxicity tests in which lower mortality was observed in larvae exposed to sGO, demonstrating that oxidative stress was one of the underlying mechanisms of acute toxicity of lGO and mlGO in *C. riparius* and that SOD is a much more sensitive indicator than LPO. These results demonstrated that the lateral dimension of GO flakes can be defined as a crucial physical parameter of this kind of material for future toxicity studies in aquatic organisms.

*C. riparius* is a keystone species in freshwater aquatic ecosystems and an essential organism in the food web, so further studies on the effects of GO types at the molecular and cellular level are essential.

### ***CRediT authorship contribution statement***

All authors contributed to the study conception and design. *Raquel Martin-Folgar*: conceptualization, writing, methodology review and editing. *Adrián Esteban-Arranz*: synthesis and characterization of carbon nanomaterials, writing, review and editing. *Viviana Negri*: characterization of carbon nanomaterials, review and editing. *Mónica Morales*: conceptualization, investigation reviewing and editing, writing original draft preparation, supervision.

### ***Acknowledgements***

This work was funded by the Programa Estatal de I+D+i Orientada a los Retos de la Sociedad (Spain), Grant RTI2013-094598-B-100, from the Ciencias y Tecnologías Medioambientales program from the Agencia Estatal de Investigación. We would like to thank Helena Dorado Monreal from the Departamento de Física Matemática y de Fluidos (UNED) for her technical support, Eduardo Prado for the HRSEM and STEM micrographs and Manuel Pancorbo Castro from the Departamento de Física de los Materiales for his technical collaboration in the photographs of *C. riparius*.

### ***Conflict of interest***

The authors declare that they have no conflicts of interest.



## References

- Anderson, T.D., Jin-Clark, Y., Begum, K., Starkey, S.R., Zhu, K.Y., 2008. Gene expression profiling reveals decreased expression of two hemoglobin genes associated with increased consumption of oxygen in *Chironomus tentans* exposed to atrazine: A possible mechanism for adapting to oxygen deficiency. *Aquat. Toxicol.* 86. <https://doi.org/10.1016/j.aquatox.2007.10.015>
- ASTM International. 2006. Standard guide for conducting acute toxicity tests on test materials with fishes, macroinvertebrates, and amphibians. E729-96 (2002), 2006. , in: *Annual Book of ASTM Standards*. Philadelphia, pp. 178–199.
- Batista de Melo, C., Côa, F., Alves, O.L., Martinez D.S.T., Barbieri, E., 2019. Co-exposure of graphene oxide with trace elements: Effects on acute ecotoxicity and routine metabolism in *Palaemon pandaliformis* (shrimp). *Chemosphere* 223. <https://doi.org/10.1016/j.chemosphere.2019.02.017>
- Benzait, Z., Chen, P., Trabzon, L., 2021. Enhanced synthesis method of graphene oxide. *Nanoscale Adv.* 3. <https://doi.org/10.1039/D0NA00706D>
- Berg, M.B., Hellenthal, R.A., 1992. The role of Chironomidae in energy flow of a lotic ecosystem. *Netherlands J. Aquat. Ecol.* 26. <https://doi.org/10.1007/BF02255277>
- Bianco, A., Cheng, H.-M., Enoki, T., Gogotsi, Y., Hurt, R.H., Koratkar, N., Kyotani, T., Monthieux, M., Park, C.R., Tascon, J.M.D., Zhang, J., 2013. All in the graphene family – A recommended nomenclature for two-dimensional carbon materials. *Carbon N. Y.* 65, 1–6. <https://doi.org/10.1016/J.CARBON.2013.08.038>
- Cano, A.M., Maul, J.D., Saed, M., Irin, F., Shah, S.A., Green, M.J., French, A.D., Klein, D.M., Crago, J., Cañas-Carrell, J.E., 2018. Trophic Transfer and Accumulation of Multiwalled Carbon Nanotubes in the Presence of Copper Ions in *Daphnia magna* and Fathead Minnow (*Pimephales promelas*). *Environ. Sci.*

- Technol. 52, 794–800. <https://doi.org/10.1021/acs.est.7b03522>
- Castillejos, E., Esteban-Arranz, A., Bachiller-Baeza, B., Rodríguez-Ramos, I., Guerrero-Ruiz, A., 2020. Reductive degradation of 2,4-dichlorophenoxyacetic acid using Pd/carbon with bifunctional mechanism. Catal. Today 357. <https://doi.org/10.1016/j.cattod.2019.09.007>
- Chen, L., Hu, P., Zhang, L., Huang, S., Luo, L., Huang, C., 2012. Toxicity of graphene oxide and multi-walled carbon nanotubes against human cells and zebrafish. Sci. China Chem. 55. <https://doi.org/10.1007/s11426-012-4620-7>
- Chen, M., Yin, J., Liang, Y., Yuan, S., Wang, F., Song, M., Wang, H., 2016. Oxidative stress and immunotoxicity induced by graphene oxide in zebrafish. Aquat. Toxicol. 174. <https://doi.org/10.1016/j.aquatox.2016.02.015>
- Chen, Y., Rivers-Auty, J., Crică, L.E., Barr, K., Rosano, V., Arranz, A.E., Loret, T., Spiller, D., Bussy, C., Kostarelos, K., Vranic, S., 2021. Dynamic interactions and intracellular fate of label-free, thin graphene oxide sheets within mammalian cells: role of lateral sheet size. Nanoscale Adv. <https://doi.org/10.1039/D1NA00133G>
- Choi, J., Ha, M.-H., 2009. Effect of cadmium exposure on the globin protein expression in 4th instar larvae of *Chironomus riparius* Mg. (Diptera: Chironomidae): An ecotoxicoproteomics approach. Proteomics 9. <https://doi.org/10.1002/pmic.200701197>
- Chupani, L., Niksirat, H., Velíšek, J., Stará, A., Hradilová, Š., Kolařík, J., Panáček, A., Zusková, E., 2018. Chronic dietary toxicity of zinc oxide nanoparticles in common carp (*Cyprinus carpio* L.): Tissue accumulation and physiological responses. Ecotoxicol. Environ. Saf. 147. <https://doi.org/10.1016/j.ecoenv.2017.08.024>
- Compton, O.C., Nguyen, S.T., 2010. Graphene oxide, highly reduced graphene oxide, and graphene: Versatile building blocks for carbon-based materials. Small 6, 711–

723. <https://doi.org/10.1002/sml.200901934>

Dai, J., Wang, G., Ma, L., Wu, C., 2015. Study on the surface energies and dispersibility of graphene oxide and its derivatives. *J. Mater. Sci.* 50, 3895–3907.

<https://doi.org/10.1007/s10853-015-8934-z>

De Coursin Jacobs, L.M., 2006. Chironomid Hemoglobin Genetic Diversity as an Indicator of the New Jersey Hackensack Meadowlands Wetland Health. Seton Hall University, Seton.

de Lázaro, I., Vranic, S., Marson, D., Rodrigues, A.F., Buggio, M., Esteban-Arranz, A., Mazza, M., Posocco, P., Kostarelos, K., 2019. Graphene oxide as a 2D platform for complexation and intracellular delivery of siRNA. *Nanoscale* 11.

<https://doi.org/10.1039/C9NR02301A>

De Marchi, L., Pretti, C., Gabriel, B., Marques, P.A.A.P., Freitas, R., Neto, V., 2018.

An overview of graphene materials: Properties, applications and toxicity on aquatic environments. *Sci. Total Environ.* 631–632, 1440–1456.

<https://doi.org/10.1016/J.SCTOTENV.2018.03.132>

ESTEBAN-ARRANZ, A., Arranz, M. Á., Morales, M., Martín-Folgar, R., Álvarez-Rodríguez, J., 2021. Thickness of graphene oxide-based materials as a control parameter. *ChemRxiv*. Cambridge: Cambridge Open Engage, This content is a preprint and has not been peer-reviewed.

<https://doi.org/10.33774/chemrxiv-2021-sp4zs>

Esteban-Arranz, A., Compte-Tordesillas, D., Muñoz-Andrés, V., Pérez-Cadenas, M., Guerrero-Ruiz, A., 2018. Effect of surface, structural and textural properties of graphenic materials over cooperative and synergetic adsorptions of two

chloroaromatic compounds from aqueous solution. *Catal. Today* 301, 104–111.

<https://doi.org/10.1016/J.CATTOD.2017.03.048>

- Esteban-Arranz, A., Pérez-Cadenas, M., Muñoz-Andrés, V., Guerrero-Ruiz, A., 2021. Evaluation of graphenic and graphitic materials on the adsorption of Triton X-100 from aqueous solution. *Environ. Pollut.* 284. <https://doi.org/10.1016/j.envpol.2021.117161>
- He, K., Chen, G., Zeng, G., Peng, M., Huang, Z., Shi, J., Huang, T., 2017. Stability, transport and ecosystem effects of graphene in water and soil environments. *Nanoscale* 9. <https://doi.org/10.1039/C6NR09931A>
- Hu, C., Wang, Q., Zhao, H., Wang, L., Guo, S., Li, X., 2015. Ecotoxicological effects of graphene oxide on the protozoan *Euglena gracilis*. *Chemosphere* 128. <https://doi.org/10.1016/j.chemosphere.2015.01.046>
- Ighodaro, O.M., Akinloye, O.A., 2018. First line defence antioxidants-superoxide dismutase (SOD), catalase (CAT) and glutathione peroxidase (GPX): Their fundamental role in the entire antioxidant defence grid. *Alexandria J. Med.* 54. <https://doi.org/10.1016/j.ajme.2017.09.001>
- Jasim, D.A., Lozano, N., Kostarelos, K., 2016. Synthesis of few-layered, high-purity graphene oxide sheets from different graphite sources for biology. *2D Mater.* 3, 14006. <https://doi.org/10.1088/2053-1583/3/1/014006>
- Jastrzębska, A.M., Kortecz, P., Olszyna, A.R., 2012. Recent advances in graphene family materials toxicity investigations. *J. Nanoparticle Res.* 14. <https://doi.org/10.1007/s11051-012-1320-8>
- Kettler, K., Veltman, K., van de Meent, D., van Wezel, A., Hendriks, A.J., 2014. Cellular uptake of nanoparticles as determined by particle properties, experimental conditions, and cell type. *Environ. Toxicol. Chem.* 33. <https://doi.org/10.1002/etc.2470>
- Kostarelos, A.F.R. and L.N. and N.L. and S.P.M. and B.F. and C.B. and K., 2018. A

- blueprint for the synthesis and characterisation of thin graphene oxide with controlled lateral dimensions for biomedicine. *2D Mater.* 5, 35020.
- Li, J., Wang, X., Mei, K.-C., Chang, C.H., Jiang, J., Liu, X., Liu, Q., Guiney, L.M., Hersam, M.C., Liao, Y.-P., Meng, H., Xia, T., 2021. Lateral size of graphene oxide determines differential cellular uptake and cell death pathways in Kupffer cells, LSECs, and hepatocytes. *Nano Today* 37. <https://doi.org/10.1016/j.nantod.2020.101061>
- Li, M., Czymmek, K.J., Huang, C.P., 2011. Responses of *Ceriodaphnia dubia* to TiO<sub>2</sub> and Al<sub>2</sub>O<sub>3</sub> nanoparticles: A dynamic nano-toxicity assessment of energy budget distribution. *J. Hazard. Mater.* 187. <https://doi.org/10.1016/j.jhazmat.2011.01.061>
- Lin, J., Zhang, H., Chen, Z., Zheng, Y., 2010. Penetration of Lipid Membranes by Gold Nanoparticles: Insights into Cellular Uptake, Cytotoxicity, and Their Relationship. *ACS Nano* 4. <https://doi.org/10.1021/nn1010792>
- Linares, J., Matesanz, M.C., Vila, M., Feito, M.J., Gonçalves, G., Vallet-Regí, M., Marques, P.A.A.P., Portolés, I.M.T., 2014. Endocytic Mechanisms of Graphene Oxide Nanosheets in Chondroblasts, Hepatocytes and Macrophages. *ACS Appl. Mater. Interfaces* 6. <https://doi.org/10.1021/am5031598>
- Lipowsky, R., Döbereiner, H.-G., 1998. Vesicles in contact with nanoparticles and colloids. *Europhys. Lett.* 43. <https://doi.org/10.1209/epl/i1998-00343-4>
- Liu, S., Zeng, T.H., Hofmann, M., Burcombe, E., Wei, J., Jiang, R., Kong, J., Chen, Y., 2011. Antibacterial Activity of Graphite, Graphite Oxide, Graphene Oxide, and Reduced Graphene Oxide: Membrane and Oxidative Stress. *ACS Nano* 5. <https://doi.org/10.1021/nn202451x>
- LIU Xiao Tong, M.X.Y.W.X.L.M.L.X.G.W.B.M.Y.Q.S.H.W.C.J.L.X.F., 2014. Toxicity of Multi-Walled Carbon Nanotubes, Graphene Oxide, and Reduced

- Graphene Oxide to Zebrafish Embryos. *Biomed. Environ. Sci.* 27, 676–683.
- López-Díaz, D., López Holgado, M., García-Fierro, J.L., Velázquez, M.M., 2017. Evolution of the Raman Spectrum with the Chemical Composition of Graphene Oxide. *J. Phys. Chem. C* 121. <https://doi.org/10.1021/acs.jpcc.7b06236>
- Lushchak, V., Semchyshyn, H., Lushchak, O., Mandryk, S., 2005. Diethyldithiocarbamate inhibits in vivo Cu,Zn-superoxide dismutase and perturbs free radical processes in the yeast *Saccharomyces cerevisiae* cells. *Biochem. Biophys. Res. Commun.* 338. <https://doi.org/10.1016/j.bbrc.2005.10.147>
- Lushchak, V.I., 2011. Adaptive response to oxidative stress: Bacteria, fungi, plants and animals. *Comp. Biochem. Physiol. Part C Toxicol. Pharmacol.* 153. <https://doi.org/10.1016/j.cbpc.2010.10.004>
- Lv, X., Yang, Y., Tao, Y., Jiang, Y., Chen, B., Zhu, X., Cai, Z., Li, B., 2018. A mechanism study on toxicity of graphene oxide to *Daphnia magna*: Direct link between bioaccumulation and oxidative stress. *Environ. Pollut.* 234, 953–959. <https://doi.org/10.1016/J.ENVIPO.2017.12.034>
- MacDonald, M.M., Warne, N.L., Stock, N.L., Mabury, S.A., Solomon, K.R., Sibley, P.K., 2004. TOXICITY OF PERFLUOROOCTANE SULFONIC ACID AND PERFLUOROOCTANOIC ACID TO *CHIRONOMUS TENTANS*. *Environ. Toxicol. Chem.* 23. <https://doi.org/10.1897/03-449>
- Majumdar TN, G.A., 2012. Acute and chronic toxicity of copper on aquatic insect *Chironomus ramosus* from Assam. *J Env. Biol* 139–142.
- Malhotra, N., Villaflores, O.B., Audira, G., Siregar, P., Lee, J.-S., Ger, T.-R., Hsiao, C.-D., 2020. Toxicity Studies on Graphene-Based Nanomaterials in Aquatic Organisms: Current Understanding. *Molecules* 25. <https://doi.org/10.3390/molecules25163618>

- Marcano, D.C., Kosynkin, D. V, Berlin, J.M., Sinitskii, A., Sun, Z., Slesarev, A., Alemany, L.B., Lu, W., Tour, J.M., 2010. Improved Synthesis of Graphene Oxide. ACS Nano 4, 4806–4814. <https://doi.org/10.1021/nn1006368>
- Martínez-Paz, P., Negri, V., Esteban-Arranz, A., Martínez-Guitarte, J.L., Ballesteros, P., Morales, M., 2019. Effects at molecular level of multi-walled carbon nanotubes (MWCNT) in *Chironomus riparius* (DIPTERA) aquatic larvae. Aquat. Toxicol. 209, 42–48. <https://doi.org/https://doi.org/10.1016/j.aquatox.2019.01.017>
- Mendonça, E., Diniz, M., Silva, L., Peres, I., Castro, L., Correia, I.B., Picado, A., 2011. Effects of diamond nanoparticle exposure on the internal structure and reproduction of *Daphnia magna*. J. Hazard. Mater. 186. <https://doi.org/10.1016/j.jhazmat.2010.10.115>
- Mesarič, T., Gambardella, C., Milivojević, T., Mainali, M., Drobne, D., Falugi, C., Makovec, D., Jemec, A., Sepčić, K., 2015. High surface adsorption properties of carbon-based nanomaterials are responsible for mortality, swimming inhibition, and biochemical responses in *Artemia salina* larvae. Aquat. Toxicol. 163. <https://doi.org/10.1016/j.aquatox.2015.03.014>
- Mu, L., Gao, Y., Hu, X., 2015. L-Cysteine: A biocompatible, breathable and beneficial coating for graphene oxide. Biomaterials 52. <https://doi.org/10.1016/j.biomaterials.2015.02.046>
- Niemuth, N.J., Curtis, B.J., Hang, M.N., Gallagher, M.J., Fairbrother, D.H., Hamers, R.J., Klaper, R.D., 2019. Next-Generation Complex Metal Oxide Nanomaterials Negatively Impact Growth and Development in the Benthic Invertebrate *Chironomus riparius* upon Settling. Environ. Sci. Technol. 53. <https://doi.org/10.1021/acs.est.8b06804>
- Niki, E., Yoshida, Y., Saito, Y., Noguchi, N., 2005. Lipid peroxidation: Mechanisms,

- inhibition, and biological effects. *Biochem. Biophys. Res. Commun.* 338.  
<https://doi.org/10.1016/j.bbrc.2005.08.072>
- No Title [WWW Document], n.d.
- OECD, 2011. Test No. 235: *Chironomus* sp., Acute Immobilisation Test.  
<https://doi.org/doi:http://dx.doi.org/10.1787/9789264122383-en>
- OECD, 2010. Test No. 233: Sediment-Water Chironomid Life-Cycle Toxicity Test Using Spiked Water or Spiked Sediment.  
<https://doi.org/doi:http://dx.doi.org/10.1787/9789264090910-en>
- OECD, 2004. Test No. 218: Sediment-Water Chironomid Toxicity Using Spiked Sediment. <https://doi.org/doi:http://dx.doi.org/10.1787/9789264070264-en>
- PANDEY, S., PARVEZ, S., SAYEED, I., HAQUE, I., BINHAFEEZ, B., RAISUDDIN, S., 2003. Biomarkers of oxidative stress: a comparative study of river Yamuna fish *Wallago attu* (Bl. & Schn.). *Sci. Total Environ.* 309.  
[https://doi.org/10.1016/S0048-9597\(03\)00006-8](https://doi.org/10.1016/S0048-9597(03)00006-8)
- Peres, N.M.R., Guinea, F., Castro Neto, A.H., 2006. Electronic properties of disordered two-dimensional carbon. *Phys. Rev. B* 73.  
<https://doi.org/10.1103/PhysRevB.73.125411>
- Petersen, E.J., Akkanen, J., Kukkonen, J. V, Weber Jr., W.J., 2009. Biological uptake and depuration of carbon nanotubes by *Daphnia magna*. *Env. Sci Technol* 43, 2969–2975.
- Pretti, C., Oliva, M., Pietro, R. Di, Monni, G., Cevasco, G., Chiellini, F., Pomelli, C., Chiappe, C., 2014. Ecotoxicity of pristine graphene to marine organisms. *Ecotoxicol. Environ. Saf.* 101. <https://doi.org/10.1016/j.ecoenv.2013.11.008>
- Rasmussen, J.B., 1985. Effects of Density and Microdetritus Enrichment on the Growth of Chironomid Larvae in a Small Pond. *Can. J. Fish. Aquat. Sci.* 42.



<https://doi.org/10.1139/f85-177>

- Rieradevall M, G.E.P.N., 1995. Chironomids in the diet of fish in Lake Banyoles (Catalonia, Spain). *Chironomids from genes to Ecosyst.* 335–340.
- Sayed, I., Parvez, S., Pandey, S., Bin-Hafeez, B., Haque, R., Raisuddin, S., 2003. Oxidative stress biomarkers of exposure to deltamethrin in freshwater fish, *Channa punctatus* Bloch. *Ecotoxicol. Environ. Saf.* 56. [https://doi.org/10.1016/S0147-6513\(03\)00009-5](https://doi.org/10.1016/S0147-6513(03)00009-5)
- Scida, K., Stege, P.W., Haby, G., Messina, G.A., García, C.D., 2011. Recent applications of carbon-based nanomaterials in analytical chemistry: Critical review. *Anal. Chim. Acta.* <https://doi.org/10.1016/j.aca.2011.02.025>
- Shih, C.-J., Lin, S., Sharma, R., Strano, M.S., Blakeshtein, D., 2012. Understanding the pH-Dependent Behavior of Graphene Oxide Aqueous Solutions: A Comparative Experimental and Molecular Dynamics Simulation Study. *Langmuir* 28, 235–241. <https://doi.org/10.1021/la203607w>
- Sohn, E.K., Chung, Y.S., Johari, S.A., Kim, T.G., Kim, J.K., Lee, J.H., Lee, Y.H., Kang, S.W., Yu, I.J., 2015. Acute toxicity comparison of single-walled carbon nanotubes in various freshwater organisms. *Biomed Res Int* 2015, 323090. <https://doi.org/10.1155/2015/323090>
- Souza, J.P., Mansano, A.S., Venturini, F.P., Marangoni, V.S., Lins, P.M.P., Silva, B.P.C., Dressler, B., Zucolotto, V., 2021. Toxicity of gold nanorods on *Ceriodaphnia dubia* and *Danio rerio* after sub-lethal exposure and recovery. *Environ. Sci. Pollut. Res.* <https://doi.org/10.1007/s11356-021-12423-w>
- Souza, J.P., Mansano, A.S., Venturini, F.P., Santos, F., Zucolotto, V., 2019. Antioxidant metabolism of zebrafish after sub-lethal exposure to graphene oxide and recovery. *Fish Physiol. Biochem.* 45. <https://doi.org/10.1007/s10695-019-00678-7>

- Souza, J.P., Venturini, F.P., Santos, F., Zucolotto, V., 2018. Chronic toxicity in *Ceriodaphnia dubia* induced by graphene oxide. *Chemosphere* 190, 218–224.  
<https://doi.org/10.1016/J.CHEMOSPHERE.2017.10.018>
- Szabo, T., Maroni, P., Szilagy, I., 2020. Size-dependent aggregation of graphene oxide. *Carbon N. Y.* 160. <https://doi.org/10.1016/j.carbon.2020.01.022>
- Țucureanu, V., Matei, A., Avram, A.M., 2016. FTIR Spectroscopy for Carbon Family Study. *Crit. Rev. Anal. Chem.* 46, 502–520.  
<https://doi.org/10.1080/10408347.2016.1157013>
- United States. Environmental Protection Agency. Office of Prevention, P. and T.S., 1996. Ecological effects test guidelines, OPPTS 850.1790. Chironomid sediment toxicity test. EPA 712-C- 96-313. . USEPA.
- Vance, M.E., Kuiken, T., Vejerano, E.P., McCornis, S.P., Hochella Jr., M.F., Rejeski, D., Hull, M.S., 2015. Nanotechnology in the real world: Redeveloping the nanomaterial consumer product inventory. *Beilstein J Nanotechnol* 6, 1769–1780.  
<https://doi.org/10.3762/bjnano.5.181>
- Wahid, M.H., Eroglu, E., Chen, X., Smith, S.M., Raston, C.L., 2013. Entrapment of *Chlorella vulgaris* cells within graphene oxide layers. *RSC Adv.* 3.  
<https://doi.org/10.1039/c3ra40605a>
- Waissi, G.C., Bold, S., Pakarinen, K., Akkanen, J., Leppänen, M.T., Petersen, E.J., Kukkonen, J.V.K., 2017. *Chironomus riparius* exposure to fullerene-contaminated sediment results in oxidative stress and may impact life cycle parameters. *J. Hazard. Mater.* 322, 301–309. <https://doi.org/10.1016/j.jhazmat.2016.04.015>
- Wibroe, P.P., Petersen, S. V., Bovet, N., Laursen, B.W., Moghimi, S.M., 2016. Soluble and immobilized graphene oxide activates complement system differently dependent on surface oxidation state. *Biomaterials* 78.

<https://doi.org/10.1016/j.biomaterials.2015.11.028>

Wu, H.C., Chang, X., Liu, L., Zhao, F., Zhao, Y., 2010. Chemistry of carbon nanotubes in biomedical applications. *J. Mater. Chem.* 20, 1036–1052.

Yang, K., Wan, J., Zhang, S., Tian, B., Zhang, Y., Liu, Z., 2012. The influence of surface chemistry and size of nanoscale graphene oxide on photothermal therapy of cancer using ultra-low laser power. *Biomaterials* 33.

<https://doi.org/10.1016/j.biomaterials.2011.11.064>

Zaaba, N.I., Foo, K.L., Hashim, U., Tan, S.J., Liu, W.-W., Voon, C.H., 2017. Synthesis of Graphene Oxide using Modified Hummers Method. Solvent Influence. *Procedia Eng.* 184. <https://doi.org/10.1016/j.proeng.2017.04.118>

Zhang, C., Chen, X., Ho, S.-H., 2021. Wastewater treatment nexus: Carbon nanomaterials towards potential aquatic ecotoxicity. *J. Hazard. Mater.* 417. <https://doi.org/10.1016/j.jhazmat.2021.125959>

Zhang, S., Gao, H., Bao, G., 2015. Physical Principles of Nanoparticle Cellular Endocytosis. *ACS Nano* 9 <https://doi.org/10.1021/acsnano.5b03184>

Zhao, J., Wang, Z., White, J.C., King, B., 2014. Graphene in the Aquatic Environment: Adsorption, Dispersion, Toxicity and Transformation. *Environ. Sci. Technol.* 48, 9995–10009. <https://doi.org/10.1021/es5022679>

Zhu, S., Luo, F., Tu, X., Chen, W.C., Zhu, B., Wang, G.X., 2017. Developmental toxicity of oxidized multi-walled carbon nanotubes on *Artemia salina* cysts and larvae: Uptake, accumulation, excretion and toxic responses. *Env. Pollut.* 229, 679–687. <https://doi.org/10.1016/j.envpol.2017.07.020>

Zhu, X., Zhou, J., Cai, Z., 2011. The toxicity and oxidative stress of TiO<sub>2</sub> nanoparticles in marine abalone (*Haliotis diversicolor supertexta*). *Mar. Pollut. Bull.* 63. <https://doi.org/10.1016/j.marpolbul.2011.03.006>

Zindler, F., Glomstad, B., Altin, D., Liu, J., Jenssen, B.M., Booth, A.M., 2016.

Phenanthrene Bioavailability and Toxicity to *Daphnia magna* in the Presence of Carbon Nanotubes with Different Physicochemical Properties. Environ. Sci.

Technol. 50. <https://doi.org/10.1021/acs.est.6b03228>

Journal Pre-proof

**Declaration of interests**

The authors declare that they have no known competing financial interests or personal relationships that could have appeared to influence the work reported in this paper.

The authors declare the following financial interests/personal relationships which may be considered as potential competing interests:

Journal Pre-proof